ACS OMEGA

Open Access

http://pubs.acs.org/journal/acsodf

Article

Synthesis and Properties of a Novel Reactive and Low-Migration-Resistant Antioxidant and Its Application in Rubber Composites

Xiaonan Wang, Chaoying Sun, Liang He, Yi Liu, Qingwei Sun, Lan Dong, and Runguo Wang*

Cite This: *ACS Omega* 2024, 9, 15401−15409

Read Online

ACCESS | Metrics & More | Article Recommendations | Supporting Information

ABSTRACT: The addition of antioxidants to rubber is one of the most economical and effective methods for delaying rubber aging. However, antioxidant migration can cause environmental pollution. To address this issue, a new reactive antioxidant was synthesized via the chemical bonding of glycidyl methacrylate (GMA) and *p*-aminodiphenylamine (PPDA). The product was characterized by Fourier-transform infrared spectroscopy, which confirmed the successful reaction between GMA and PPDA, resulting in a compound with the expected structure. The mixture was then combined with a composite of styrene−butadiene rubber and carbon black. The tensile strength, antioxidant properties, migration, and RPA of the resulting materials were tested and compared with those of the commercial antioxidants *N*-(1,3-dimethylbutyl)-*N*′-phenyl-*p*-phenylenediamine, *N*-isopropyl-*N*′-phenyl-1,4-phenylenediamine, and poly(1,2-dihydro-2,2,4-trimethylquinoline). After the glycidyl methacrylate antioxidant was grafted onto *p*-aminodiphenylamine, it became highly compatible with and dispersed in the rubber matrix. The antiaging and antimigration properties of the rubber antioxidants were enhanced without damaging the mechanical properties of the rubber matrix. The short-term and long-term antiaging and antimigration properties of this antioxidant are superior to those of commercially available antioxidants.

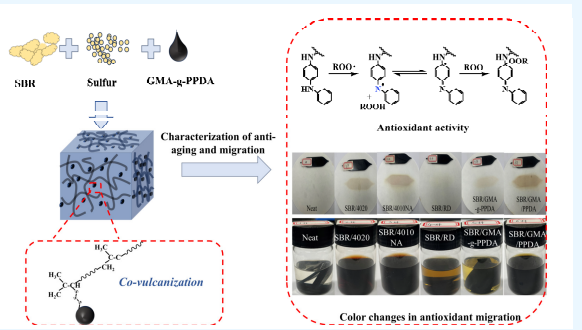

1. INTRODUCTION

Rubber is an important material with excellent elasticity, strength, toughness, and strain performance.[1,2] Rubber serves as a significant resource for human use, and with the increasing number of rubber types, the production and consumption of rubber products have surged. Rubber products play a significant role in automobiles, conveyor belts, seals, rubber shoes, and other areas of daily life.[3] Rubber products also serve critical functions in the military, aerospace, and other national defense fields. Nevertheless, the exposure of rubber products to oxygen, high or low temperatures, light, and other factors may cause the cross-linking or breakage of the polymer chains, resulting in material discoloration, whitening, softness, stickiness, hardness, brittleness, surface cracks, and other issues.[4−6] This phenomenon is known as rubber material aging, to which unsaturated rubber is particularly susceptible.[7,8]

Thermal oxidative aging is the most frequent type of rubber degradation. To delay or prevent this process, antioxidants can be added to rubber compounds during mixing.[9] Antiaging agents react primarily with the free radicals or hydrogen peroxide generated during rubber aging.[10] This reaction reduces the number of free radicals and potentially prevents the formation of active peroxide free radicals, which, in turn, slows the process. Consequently, the reaction between the rubber molecular chains and free radicals is delayed or avoided, leading to a reduction in rubber aging.[11−13] However, the widely used antioxidants typically have relatively low molecular weights. Physical depletion may occur during processing, especially at high temperatures or in liquids, resulting in reduced antioxidant effectiveness.[14] Owing to volatilization, migration, and extraction, small molecules of antioxidants in rubber materials evaporate from the product and penetrate outward, eventually migrating to the product's surface.[15−19] The precipitation of antioxidants decreases their protective effect, which leads to diminished performance and a shorter service life for the materials. Moreover, antioxidant migration pollutes the environment.[20,21] The table indicating the toxicity and chronicity of commercial antioxidants is shown in Table S1.

One common approach to address antioxidant migration is to increase their relative molecular weight.[22−25] Luo et al.[26] developed an accelerator, BTC (the structure is shown in Table S2), via a thiol−ene click chemical reaction involving *N*-4-(anilinophenyl)maleimide (antiaging agent MC) and 2-

Received: December 23, 2023
Revised: February 29, 2024
Accepted: March 4, 2024
Published: March 22, 2024

mercaptobenzothiazole (accelerator MBT). BTC was subsequently incorporated into styrene−butadiene rubber to create rubber composites. Through experimentation and molecular simulations, it was determined that the SBR/BTC composites exhibited high vulcanization efficiency, excellent mechanical properties, and strong resistance to thermal oxidative aging. Shi et al.[27] prepared a reactive antioxidant, acyl chloride hindered phenol (HP-Cl), by modifying the phenolic antioxidant triethylene glycol bis(3-*tert*-butyl-4-hydroxy-5-methylphenyl)propionate (Irganox 245). To produce HP-Cl, HP-COOH was first prepared via the hydrolysis of Irganox 245, followed by a reaction with thionyl chloride. They prepared PA 6-*g*-HP by grafting HP-Cl onto the molecular chain of PA 6 via reactive extrusion. The PA 6-*g*-HP sample exhibited a lower thermo-oxidative degradation rate constant than the PA 6/Irganox 245 sample. Moreover, the antioxidants in the PA 6/Irganox 245 sample migrated faster, resulting in higher equilibrium migration concentrations. The reactive antioxidant HP-Cl, prepared beforehand, exhibited exceptional resistance to thermal and oxidative aging and migration. Through a two-step synthesis process, Lu[28] developed a reactive antioxidant, NAPM, added it to natural rubber, and discovered that its aging resistance was superior to those of 4010NA and 4020. Zhao et al.[16] grafted the antioxidant intermediate RT onto the surface of lignin and created a hybrid modified lignin-based filled antioxidant named Lig-*g*-RT. The team compared the results with those obtained using a commercial antioxidant, 4020-stabilized SBR sulfate. The SBR sulfide salt filled with 10 phr Lig-*g*-RT achieved the best performance for thermal oxidative aging, comparable to that of the commercial antioxidant 4020. The modified Lig-*g*-RT offered synergistic intramolecular antiaging benefits to SBR sulfides, enhanced filler dispersion, and significantly broadened the industrial applicability of lignin. Therefore, increasing the molecular weight of antioxidants while incorporating reactive functional groups could be a viable approach to inhibiting their migration and enhancing their protective effectiveness in rubber matrices.

GMA-*g*-PPDA was successfully synthesized through the epoxy amination reaction.[16,29] The introduction of C═C groups into the antioxidant structure can increase its molecular weight and allow it to covulcanize with rubber, resulting in the synthesis of a new type of reactive antioxidant with a high molecular weight. We evaluated the thermal oxygen-aging resistance of the SBR/GMA-*g*-PPDA composite and investigated its role in the antioxidant behavior and migration resistance of the SBR matrix.

2. EXPERIMENTS

2.1. Materials. The glycidyl methacrylate (GMA) and *p*-aminophenylenediamine (PPDA) were supplied by Alfa Aesar. Neutral alumina was supplied by Aladdin, and styrene−butadiene rubber was purchased from Jilin Chemical Company. The remaining rubber components, including zinc oxide (ZnO), stearic acid (SA), sulfur (S), accelerator CZ, accelerator DM, and carbon black N330 (CB), were industrial-grade products.

2.2. Synthesis of Migration-Resistant Antioxidant GMA-*g*-PPDA. The synthesis pathway for GMA-*g*-PPDA is shown in Figure. 1 The specific steps involved are as follows: A 100 mL round-bottom three-necked flask was placed into an oil bath. A condenser tube and thermometer were mounted on the flask before adding purified GMA and PPDA sequentially.

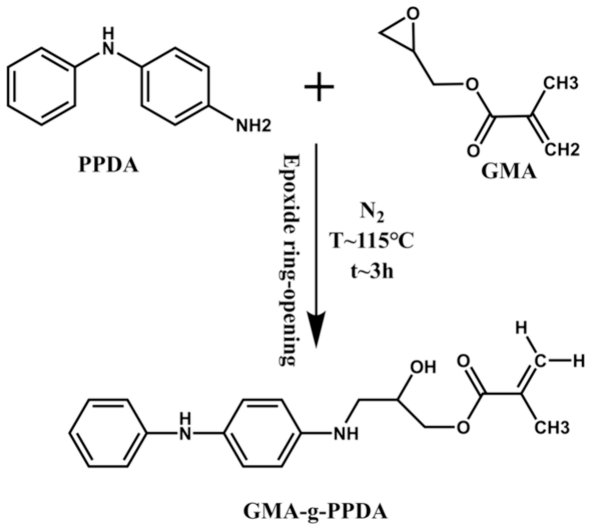

Figure 1. Epoxy addition reaction between GMA and PPDA.

A magnetic stirrer was added, and stirring was started until complete dissolution. Nitrogen gas should be continuously introduced, and the mixture should be stirred throughout the reaction process, followed by an increase in temperature. After the system reached the reaction temperature, timing was initiated. The antioxidant GMA-*g*-PPDA was obtained after a specific duration.

2.3. Preparation of Styrene−Butadiene Rubber Composites. Different antioxidant/SBR samples were prepared in a two-roll open mill using conventional mixing techniques at room temperature in accordance with the basic formula presented in Table 1. The vulcanizing agent,

Table 1. Constituents of SBR/Antioxidant Composites

Material	phr
SBR	100
Carbon Black(N330)	30
SA	2
ZnO	5
CZ	1.5
DM	0.5
S	2

accelerator, and activator dosage for the antioxidant/SBR composite materials remained consistent: CB, 30 phr; zinc oxide, 5 phr; SA, 2 phr; CZ, 1.5 phr; DM, 0.5; and S, 2 phr. GMA-*g*-PPDA was added as an antioxidant to antioxidant/SBR composite materials and compared with traditional small-molecule rubber antioxidants. Approximately 5 g of SBR compound was used to conduct a vulcanization test in a 150 °C rotorless vulcanizer. The corresponding vulcanization parameters included the vulcanization time t_{10}, positive vulcanization time t_{90}, minimum torque M_L, and maximum torque M_H. Then, the mixed rubber was vulcanized for t_{90}+2 min on a flat vulcanizer at 150 °C and 15 MPa to obtain an antioxidant/SBR vulcanized composite material. Finally, a cutter was used to cut the SBR composite material into dumbbell-shaped splines to test its mechanical and thermal oxidative aging properties.

2.4. Characterization. Fourier-transform infrared spectroscopy was performed using an infrared spectrometer (TENSOR-27, Germany). The samples were evenly mixed

https://doi.org/10.1021/acsomega.3c10301
ACS Omega 2024, 9, 15401−15409

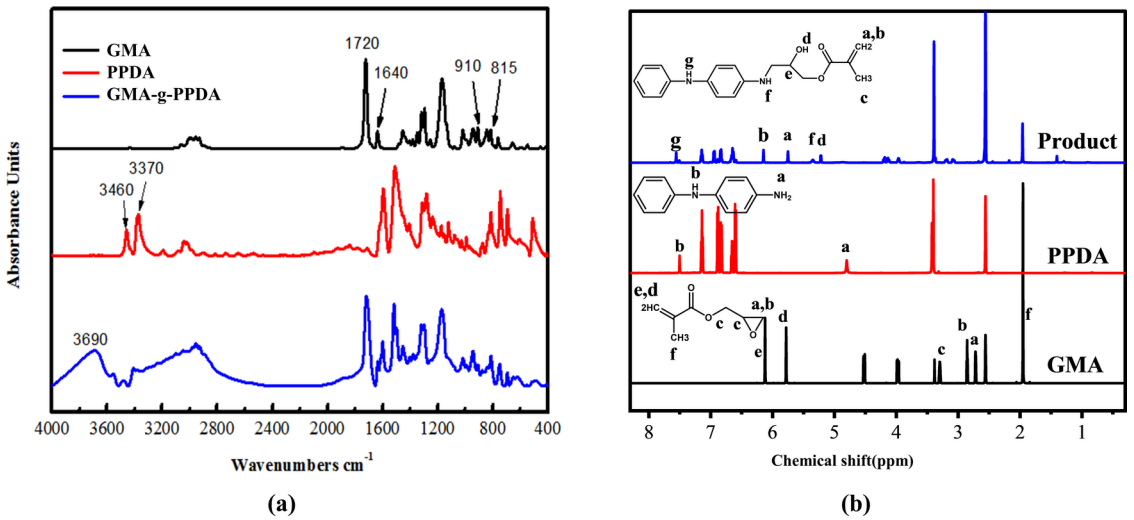

Figure 2. (a) FT-IR spectra and (b) ^{1}H NMR spectra of GMA, PPDA, and GMA-*g*-PPDA.

with potassium bromide and pressed using a tablet press for 15 s. The samples were subjected to infrared testing in the wavenumber range of 400−4000 cm^{-1}. A Bruker AV400 spectrometer was used to collect ^{1}H NMR spectra, and deuterated dimethyl sulfoxide was used as the solvent. The mixed rubber strain scanning test conditions were as follows: temperature 60 °C, frequency 1 HZ, and strain range 0−200% to test the dynamic modulus. The strain scanning test conditions of vulcanized rubber were as follows: frequency 10 HZ, strain scanning range 0−40%, and vulcanization temperature 150 °C; the vulcanization time was calculated based on the vulcanization performance parameters obtained from the test. The relative molecular weight was determined by liquid chromatography−mass spectrometry (Xevo G2 Qtof, Waters). DSC (Germany NETZSCH Company) was used to measure the oxidation exothermic peak temperature T_O of the SBR composite material under an O_2 atmosphere, with a heating rate of 10 °C·min^{-1} from 30 to 300 °C. A tensile testing machine was used to evaluate the performance of the samples. The tensile machine model was a high-speed rail testing instrument (AI-7000S1) with a tensile speed of 500 mm/min, and the data were the average value. The vulcanized rubber was tested using a GT-7014-E thermal aging oven produced by Gaotie Testing Instrument Co., Ltd. The vulcanized rubber was cut into dumbbell-shaped specimens for tensile testing, and the experimental specimens were hung vertically in an aging oven at a temperature of 100 °C. The dynamic mechanical analysis (DMA) of SBR composites was performed using a Q800 DMA thermal analyzer (TA Instruments, USA). Scanning electron microscopy (SEM) (Hitachi S-4800, Japan) was used to observe the surface morphology of the SBR composites before and after thermal oxidation. A UV−visible spectrophotometer (Agilent Company, model 8453) was used to test the absorbance of the configured standard known concentration antioxidants and to establish an absorbance−concentration relationship curve. The liquid to be tested and the ethanol solution were placed in two cuvettes, respectively, and the test range was 200−400 cm^{-1}.

3. RESULTS AND DISCUSSION

3.1. Structural Characterization of the Antioxidant GMA-*g*-PPDA. The FT-IR spectra of GMA, PPDA, and GMA-*g*-PPDA are shown in Figure 2(a). For *p*-aminodiphenylamine, there was a relatively strong double peak in the 3370−3460 cm^{-1} range, which was attributed to the stretching vibration absorption peaks of −NH and −NH$_2$. In the figure, the peak band of glycidyl methacrylate was located at 2900−3040 cm^{-1} and belonged to the stretching vibration of −CH$_3$ and −CH$_2$. The absorption peak of the carbonyl group was located at 1720 cm^{-1}, and the stretching vibration of the unsaturated double bond was located at 1640 cm^{-1}. The epoxy skeleton was characterized by vibration absorption peaks at 910, 844, and 815 cm^{-1}. The grafting of glycidyl methacrylate to *p*-aminodiphenylamine produced a distinct broad peak within the 3300−3650 cm^{-1} range, which corresponded to the vibration absorption peak resulting from the −OH generated during the epoxy ring-opening grafting reaction and the characteristic absorption peaks of certain secondary amines (−NH). Additionally, the spectrum displays the stretching vibration absorption peaks of the C═O (1720 cm^{-1}) and C═C double bonds (1638 cm^{-1}). Therefore, we successfully prepared *para*-aminodiphenylamine modified with a glycidyl methacrylate graft using glycidyl methacrylate.

The ^{1}H NMR spectra in Figure 2(b) provide further evidence for the reaction between GMA and PPDA. The NMR spectrum for GMA-*g*-PPDA, the chemical reaction product, demonstrated that there was no signal peak at 4.77 in the product spectrum, indicating that all primary amines on *p*-aminodiphenylamine (PPDA) were involved in the reaction and fully consumed. New signal peaks appeared in the NMR spectrum of the product at chemical shifts of 5.15 and 5.29 ppm, corresponding to the hydroxyl hydrogen signal peaks produced by the ring-opening of epoxy. The hydroxyl hydrogen on the carbon atom connected to the hydroxyl group was identifiable in the product spectrum. The hydrogen peak signal provided additional evidence that the reaction acknowledged the epoxy character of the amino group and underwent a ring-opening reaction to yield the hydroxyl group.

Moreover, the mass spectrum displayed in Figure 3 illustrates that the mass-to-charge ratio (m/z) at the most prominent peak was 327, which is consistent with the theoretical molecular weight of GMA-*g*-PPDA. These results implied that GMA-*g*-PPDA was effectively synthesized through the reaction of GMA with PPDA.

https://doi.org/10.1021/acsomega.3c10301
ACS Omega 2024, 9, 15401−15409

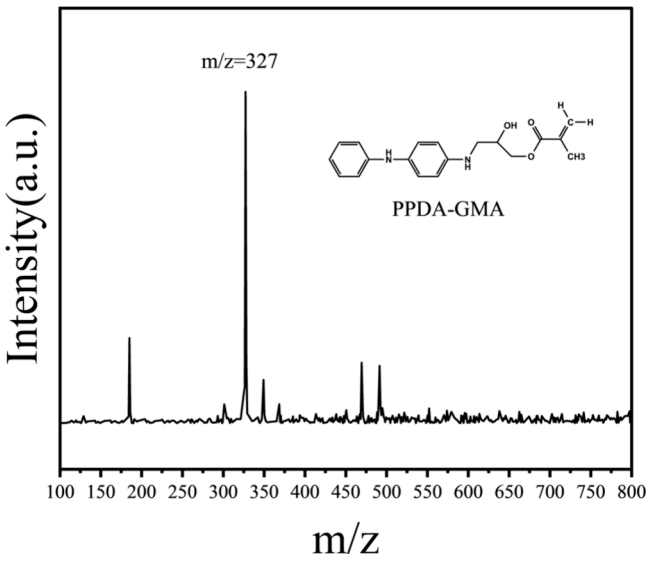

Figure 3. Mass spectrum of GMA-*g*-PPDA under the anode ionization mode.

3.2. Vulcanization and Mechanical Properties of Styrene−Butadiene Rubber Composites. Figure 4(a) shows the vulcanization characteristic curve of the antioxidant/SBR compound. The corresponding vulcanization parameters are listed in Table 2. The scorch time t_{10} of GMA-*g*-PPDA/SBR was shorter than those of 4010NA/SBR and 4020/SBR. The positive vulcanization time t_{90} of GMA-*g*-PPDA/SBR was shorter than that of 4010NA/SBR and 4020/SBR. Both t_{10} and t_{90} were shorter than 4010NA/SBR and 4020/SBR, respectively. This is because the antiaging agent GMA-*g*-PPDA contained both hydroxyl and weakly alkaline amine structures, which are similar in structure to the more active alcohol amine surfactants. The antiaging agent GMA-*g*-PPDA can play a similar activation role, improve the vulcanization system, cause the vulcanization reaction to proceed as early as possible, and decrease t_{10}, thereby increasing the vulcanization speed and decreasing t_{90}. The GMA-*g*-PPDA/SBR sample had shorter t_{10} and t_{90}, which is beneficial for the efficient processing of rubber products.[30] As shown in Figure 4(b), the impact of the addition of GMA-*g*-PPDA on the mechanical properties of rubber was similar to that of commercial antioxidants.

Table 2. Vulcanization Characteristic Data of Different Composite Materials

Sample	T_{10} (min)	T_{90} (min)	M_H (dN·m)	M_L (dN·m)
Neat	3:11	33:01	11.50	1.79
SBR/4020	3:48	21:07	11.89	1.74
SBR/4010NA	2:51	28:56	11.46	1.79
SBR/RD	3:02	32:07	11.67	1.82
SBR/GMA-*g*-PPDA	2:25	18:28	12.17	1.76
SBR/GMA/PPDA	1:51	26:49	11.90	1.70

3.3. Processing Properties of Styrene−Butadiene Rubber Composite Materials. Figure 5(a) shows the relationship between the storage modulus and strain of the compound rubber, which is typically used to characterize the dispersion of fillers in rubber. The higher storage modulus G' and larger storage modulus change indicate that the filler was poorly dispersed. It can be seen from the figure that the rubber composite material with 4020 had a lower storage modulus, whereas the storage modulus of the rubber composite material with GMA-*g*-PPDA was slightly higher. This is because the presence of −OH in the antioxidant structure could adsorb or combine with carbon black, causing tiny aggregations of fillers, strengthening the filler−filler network, and reducing the dispersion of fillers.

Figure 5(b) shows several sets of vulcanized rubber loss factor−strain relationship curves. The loss factor of the rubber composite with antioxidant GMA-*g*-PPDA was slightly higher than that of the rubber composite with 4020. The antioxidant GMA-*g*-PPDA had double bonds that covulcanized with the rubber matrix, resulting in a decrease in cross-linking density. The reduction in cross-linking points is equivalent to reducing the "binding" between rubber molecular chains, making the molecular chains easier to move, resulting in periodic movement of rubber, in which more heat is dissipated and the loss factor value increases. The −OH in the antioxidant structure will adsorb or combine with the carbon black, resulting in tiny aggregation, which will increase the friction between filler and filler and between filler and rubber, causing tan δ to rise. This indirectly indicates that GMA-*g*-PPDA is involved in rubber vulcanization.

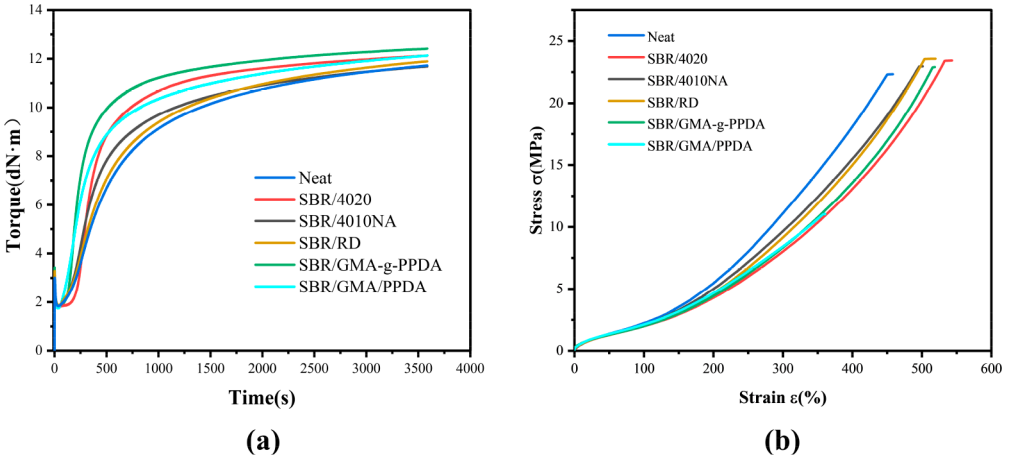

Figure 4. (a) Cure characteristics of different SBR composites and (b) stretch curves of SBR composites.

https://doi.org/10.1021/acsomega.3c10301
ACS Omega 2024, 9, 15401−15409

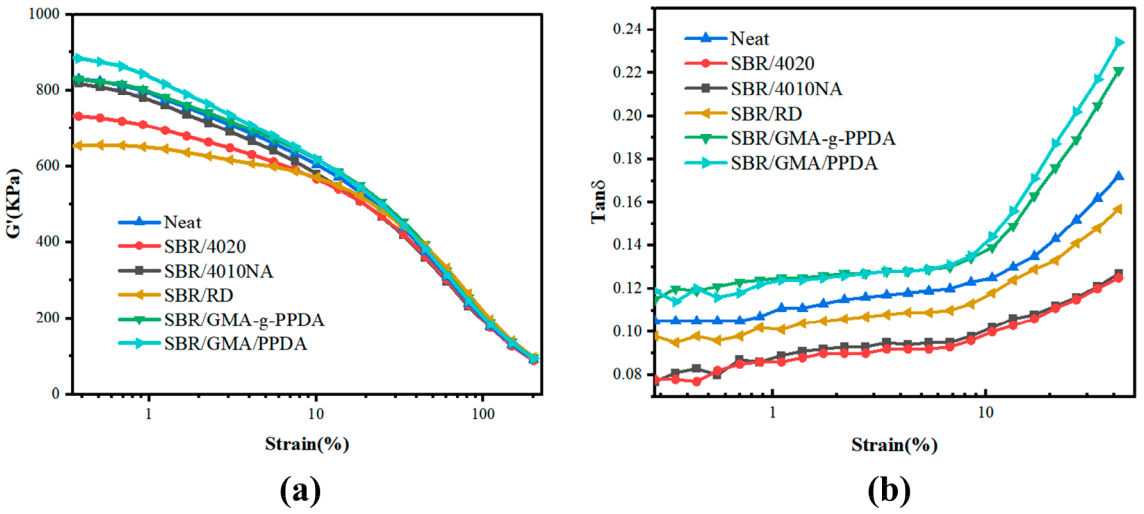

Figure 5. (a) Strain dependence of G' for different styrene−butadiene rubber composites and (b) dissipation tan δ-strain curve of the styrene−butadiene rubber composite.

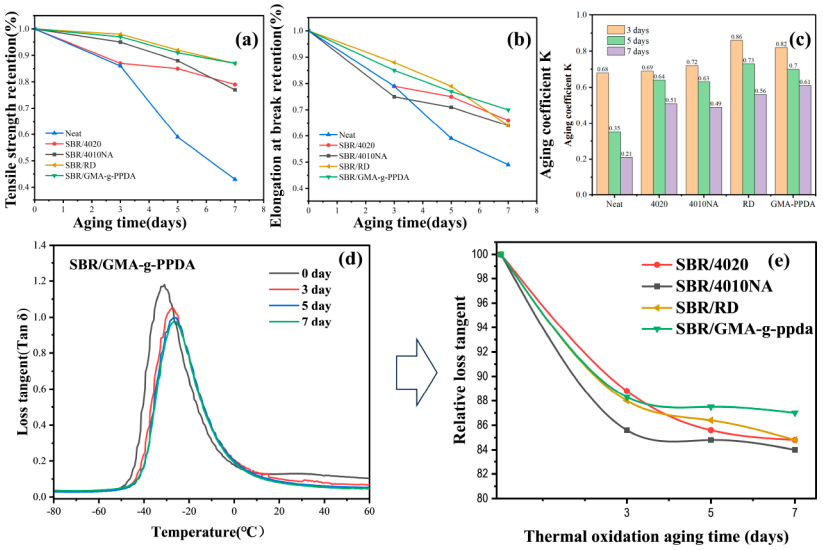

Figure 6. (a) Curve of vulcanized rubber tensile strength and (b) elongation at break retention rate with aging time. (c) Aging coefficient K of SBR composites. (d) DMA curves of tan δ with temperature for SBR/GMA-g-PPDA obtained during aging at 100 °C for various days. (e) Relative peak value of tan δ with thermal oxidation aging time.

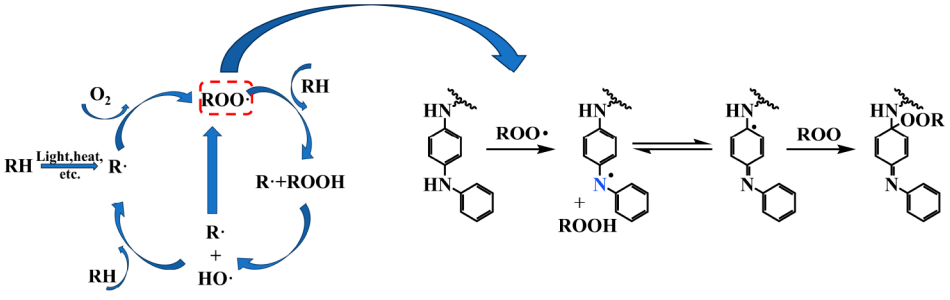

Figure 7. Rubber auto-oxidation mechanism and action mechanism of free radicals and antioxidants.

3.4. Thermo-oxidative Aging Resistance of SBR Composites. Mechanical properties are crucial for the effective utilization of rubber products. However, exposure to heat and oxygen increases the cross-linking density within the rubber, leading to a decline in the mechanical properties of the SBR composite material. Testing the changes in the mechanical properties of SBR composite materials during the aging process can characterize their aging resistance. Figure 6(a) and (b) illustrates the retention rates of the tensile strength and elongation at break of the SBR composites before and after aging. Meanwhile, Figure 6(c) shows the calculated aging coefficients of different SBR composite materials. The

https://doi.org/10.1021/acsomega.3c10301
ACS Omega 2024, 9, 15401−15409

images indicate that the tensile strength and elongation at break decreased significantly after aging. However, SBR/GMA-*g*-PPDA exhibited the highest *K* value among the antioxidants under identical aging conditions, indicating that the SBR/GMA-*g*-PPDA composites demonstrated exceptional stability. During the rubber aging process, continuous aging occurred as new free radicals were generated after the initial ones, as shown in Figure 7. The antioxidant GMA-*g*-PPDA swiftly captured free radicals and avoided outward migration, resulting in long-term antioxidant effects.

In addition, DMA can be used to measure the dynamic mechanical properties of viscoelastic materials under varying frequencies, temperatures, and loads. In this study, we analyzed the chain motion during the aging of SBR composites by testing the dynamic mechanical properties of the SBR/antioxidant composites at different aging times. Figure 6(d) displays the variation curve of tan δ with the temperature of the SBR/GMA-*g*-PPDA composite, while Figure 6(e) depicts the tan δ value and retention rate of SBR composites. After undergoing aging, the rubber chains within the SBR composite material become cross-linked, leading to a decline in its dynamic mechanical properties and a gradual reduction in the value of tan δ.[31] Compared with other SBR composites, the rate of decrease in the tan δ value of SBR/GMA-*g*-PPDA composites was lower. Thus, the antioxidant GMA-*g*-PPDA exhibited superior resistance to thermal oxidative aging.

3.5. Temperature at the Oxidation Exothermic Peak (T_O). The oxidation induction period (OIP) test is commonly used to quantify the extent of degradation of polymers, such as rubber or plastic, under specific testing conditions. The OIP test duration indicates the time required for the material to undergo autocatalytic oxidation triggered by exposure to high-temperature-oxygen conditions.[32] The greater the OIT value, the greater the resistance of the material to oxidative degradation.[33] Figure 8 shows the DSC curve of the SBR/antioxidant composite material under an oxygen atmosphere. The T_O temperature of the SBR composites with added antioxidants was higher than that of the composites without antioxidants, indicating that the addition of antioxidants could slow the thermal oxidative aging of SBR composites. As an antioxidant, GMA-*g*-PPDA can effectively improve the antioxidant degradation ability of the SBR composites, and its effect is superior to that of other commercial antioxidant systems.

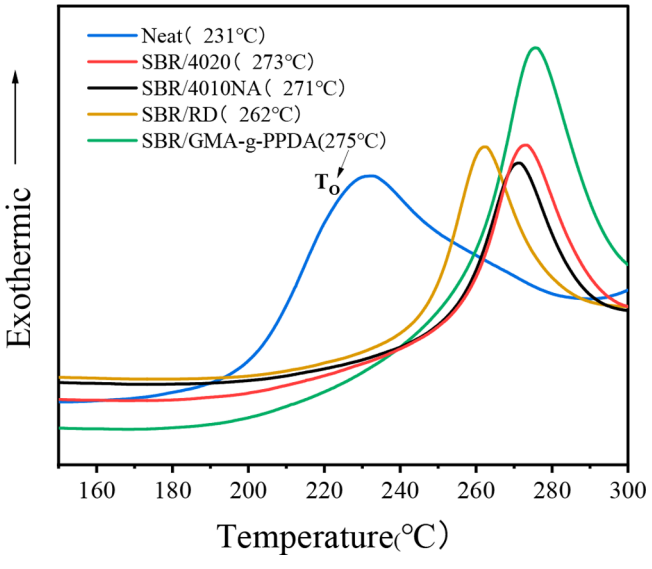

Figure 8. DSC curves of SBR/antioxidant composites.

3.6. Surface Morphology of SBR/Antioxidant Composite Materials. Figure 9 shows that no surface defects are visible on the different SBR/antioxidant composites after 3 and 5 days of aging. Nevertheless, with increased aging time and the erosion effects of heat and oxygen, defects emerged on the surface of the SBR/4020 composite after 9 days. Similarly, defects were observed on the surfaces of the SBR/4010NA and SBR/RD samples. However, GMA-*g*-PPDA, which exists in the form of black oil, functions as a plasticizer during thermo-oxidative aging and demonstrates highly effective and enduring protective traits by rapidly reacting with and capturing the generated free radicals.

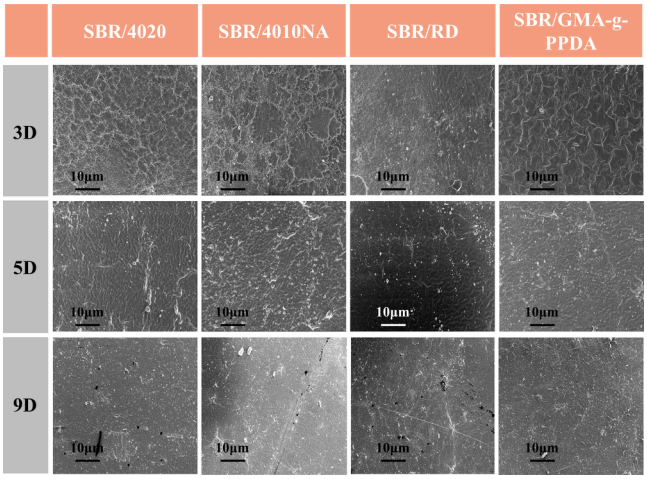

Figure 9. SEM images of the surface of SBR/antioxidant composite materials under 3 days, 5 days, and 9 days.

3.7. Migration of Antioxidants in the SBR Matrix. *3.7.1. Extraction and Accelerated Migration.* In the previous section, we examined the resistance of the GMA-*g*-PPDA antioxidants to thermal oxygen aging. Migration resistance was the primary focus of this study. Solvent extraction was used to simulate the migration of the antioxidants within the liquid medium. This method imitates the migration process. The method of accelerating migration by placing rubber on the filter paper simulates the migration of antioxidants between interfaces.

Figure 11 displays the alteration in the color of the vulcanized rubber samples with the same mass soaked in the same volume of ethanol at the initial soaking state and after 7 and 30 days of soaking. The migration resistance of the antioxidants was characterized by observing the color change of the solution. After 30 days of soaking, the color of multiple-antioxidant rubber composites from the commercial sector soaked in ethanol was compared with the color of rubber composites with the added antioxidant GMA-*g*-PPDA that were also soaked in ethanol. Rubber composites containing antioxidants 4020 and 4010NA were immersed and extracted, resulting in solutions that were noticeably darker in color than those of the rubber composites with GMA-PPDA antioxidants, which had also been immersed. As shown in Figure 10, the antioxidant GMA-*g*-PPDA has reactive groups, such as double bonds, which form chemical bonds with the rubber molecular

https://doi.org/10.1021/acsomega.3c10301
ACS Omega 2024, 9, 15401−15409

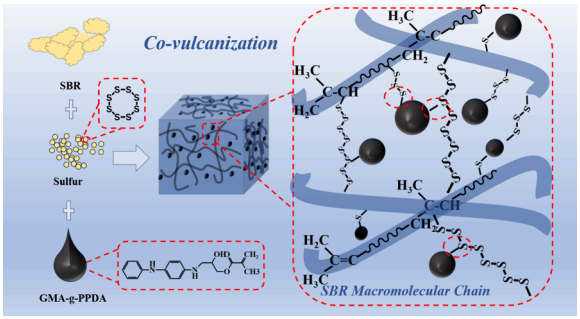

Figure 10. Schematic diagram of GMA-*g*-PPDA/SBR covulcanization.

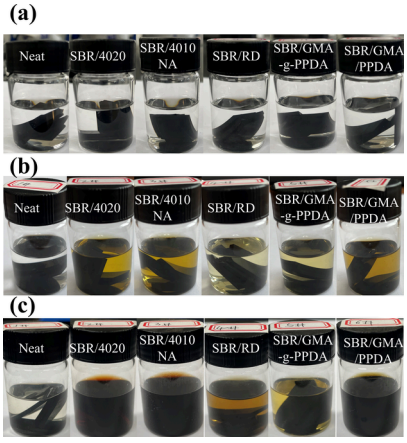

Figure 11. Color change of ethanol after soaking vulcanizate.

chain during vulcanization. The molecular weight of the antioxidant GMA-*g*-PPDA exceeded those of 4020 and 4010NA. As a result, GMA-PPDA had better migration resistance than antioxidants 4020 and 4010NA. The migration resistance of SBR/GMA-*g*-PPDA was significantly higher than that of SBR/GMA/PPDA, indicating that the chemical bonding between GMA and PPDA could greatly enhance the migration of PPDA.

The samples were placed in an oven to expedite antioxidant migration. After 1 week, we found that the color of the filter paper was changed. The test was conducted at the temperature of 60 °C, and the corresponding results are presented in Figure 12. The rubber composites containing the antioxidants 4020, 4010NA, and GMA/PPDA resulted in darker colors on the filter paper. Rubber composites supplemented with the GMA-*g*-PPDA antioxidant produced only faint hues on the filter paper. This result differs from the extraction results. The color

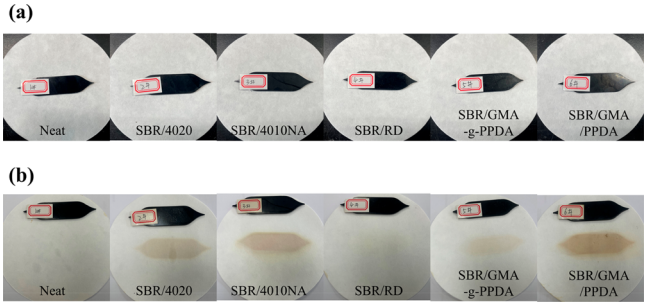

Figure 12. Color change of filter paper (a) before and (b) after aging.

of SBR/GMA-*g*-PPDA was somewhat darker than that of SBR/RD because of the migration of unreacted PPDA.

3.7.2. Elemental Quantitative Analysis. A quantitative study was conducted using a UV spectrophotometer. Equal weights of vulcanized rubber were immersed in methanol of identical mass. After a 60 h soaking period, the concentration of the antioxidants in the methanol solution was quantified.

To prepare a standard concentration solution of antioxidants in ethanol, we analyzed the absorbance using a UV spectrophotometer, established the relationship between the absorbance and concentration of antioxidants, and calculated the antioxidant concentration in the ethanol solution using the relationship curve. The standard concentrations were 2.5, 5, 10, 20, and 40 mg/L.

The UV−visible absorbance of ethanol at 200−400 nm after soaking the vulcanized rubber is shown in Figure 13 The

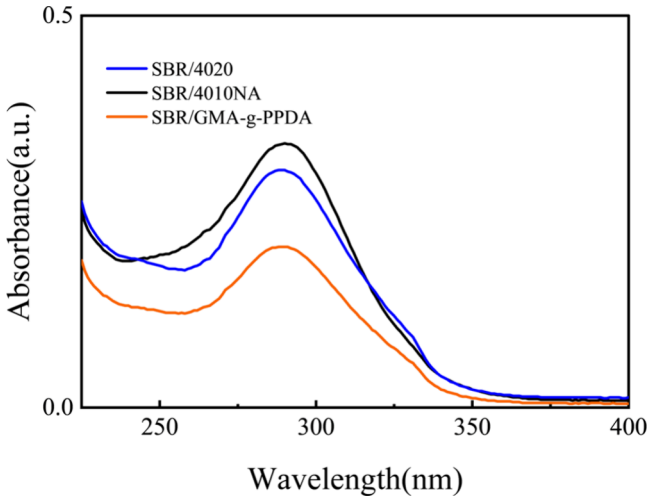

Figure 13. UV−vis absorbance of ethanol solution after immersion of vulcanized rubber.

concentrations of the antioxidants that migrated into the ethanol solution were calculated, as shown in Table 3. After

Table 3. Absorbance and concentration of ethanol solutions immersed in different vulcanizates

Sample	Absorbance	Concentration/10^{-2} g/L
4010NA	0.336	1.960
4020	0.303	1.806
GMA-*g*-PPDA	0.205	1.305

soaking for 60 h, the concentrations of antioxidants 4020 and 4010NA in the ethanol solution were higher than those of antioxidant GMA-*g*-PPDA, indicating that antioxidant GMA-*g*-PPDA had better solvent extraction resistance than antioxidants 4020 and 4010NA.

Table 4 shows the surface nitrogen content of the different composite materials before and after aging. The aging time was 3 days. The relative contents of the rubber surface elements were measured using XPS. The table shows the relative contents of the surface nitrogen elements in the three groups of samples before and after aging. Before aging, the surface nitrogen content of the styrene−butadiene rubber composite with the modified antioxidant GMA-*g*-PPDA was 1.62%, which was between those of 4020 and 4010NA. The surface nitrogen content of SBR/GMA-*g*-PPDA after aging increased by 18.5%

https://doi.org/10.1021/acsomega.3c10301
ACS Omega 2024, 9, 15401−15409

Table 4. Nitrogen Contents of Different Composite Materials before and after Aging

Sample	Before aging	After aging	Nitrogen content increase rate
4010NA	1.60%	1.98%	23.8%
4020	1.64%	2.04%	24.4%
GMA-*g*-PPDA	1.62%	1.92%	18.5%

compared with that before aging, which was lower than the increase rate of the two control groups. This indicates that the modified antioxidant GMA-*g*-PPDA was more effective than the other antioxidants during the aging process.

4. CONCLUSIONS

In this study, a new reactive antioxidant, GMA-*g*-PPDA, was successfully synthesized via the epoxy amination of GMA and PPDA. The antioxidant GMA-*g*-PPDA exhibited outstanding long-term thermal oxygen protection properties and exemplary migration resistance. Moreover, the GMA-*g*-PPDA was environmentally friendly. The antioxidant GMA-*g*-PPDA contained double bonds. These bonds enable a covulcanization reaction with the rubber matrix, resulting in grafting onto molecular chains. This resulted in the notable preservation of GMA-*g*-PPDA within the SBR matrix, leading to improved resistance to antioxidant migration. Therefore, we anticipate that this study will offer novel insights into the development of eco-friendly and effective antioxidants for rubber manufacturing.

■ ASSOCIATED CONTENT

Supporting Information

The Supporting Information is available free of charge at https://pubs.acs.org/doi/10.1021/acsomega.3c10301.

Evaluation of HSE characteristics based on GHS classification. Molecular structures of all the antioxidants reviewed in this paper (PDF)

■ AUTHOR INFORMATION

Corresponding Author

Runguo Wang − *Beijing Engineering Research Center of Advanced Elastomers, Beijing University of Chemical Technology, Beijing 100029, China;* orcid.org/0000-0002-0583-6152; Email: wangrg@mail.buct.edu.cn

Authors

Xiaonan Wang − *Beijing Engineering Research Center of Advanced Elastomers, Beijing University of Chemical Technology, Beijing 100029, China*

Chaoying Sun − *Beijing Engineering Research Center of Advanced Elastomers, Beijing University of Chemical Technology, Beijing 100029, China*

Liang He − *Beijing Engineering Research Center of Advanced Elastomers, Beijing University of Chemical Technology, Beijing 100029, China*

Yi Liu − *Beijing Engineering Research Center of Advanced Elastomers, Beijing University of Chemical Technology, Beijing 100029, China*

Qingwei Sun − *Beijing Engineering Research Center of Advanced Elastomers, Beijing University of Chemical Technology, Beijing 100029, China*

Lan Dong − *Beijing Engineering Research Center of Advanced Elastomers, Beijing University of Chemical Technology, Beijing 100029, China*

Complete contact information is available at: https://pubs.acs.org/10.1021/acsomega.3c10301

Author Contributions

All authors have given approval to the final version of the manuscript.

Notes

The authors declare no competing financial interest.

■ ACKNOWLEDGMENTS

Over the course of the researching and writing of this paper, X.W. expresses thanks to all those who have helped him. A special acknowledgment should be shown to Professor Runguo Wang. X.W. is particularly indebted to Chaoying Sun, Liang He, Yi Liu, Qingwei Sun, and Lan Dong who gave kind encouragement and useful instructions all through the writing.

■ REFERENCES

(1) Qiao, H.; Chao, M.; Hui, D.; Liu, J.; Zheng, J.; Lei, W.; Zhou, X.; Wang, R.; Zhang, L. Enhanced interfacial interaction and excellent performance of silica/epoxy group-functionalized styrene-butadiene rubber (SBR) nanocomposites without any coupling agent. *Compos. B. Eng.* **2017**, *114*, 356−364.

(2) Wu, W.; Zeng, X.; Li, H.; Lai, X.; Li, F.; Guo, J. Synthesis and Characterization of A Novel Macromolecular Hindered Phenol Antioxidant and Its Thermo-Oxidative Aging Resistance for Natural Rubber. *J. Macromol. Sci. Phys, part b* **2014**, *53* (7), 1244−1257.

(3) Matchawet, S.; Nakason, C.; Kaesaman, A. Electrical and Mechanical Properties of Conductive Carbon Black Filled Epoxidized Natural Rubber. *Adv. Mat Res.* **2013**, *844*, 255−258.

(4) Chai, R. D.; Chen, S. J.; Zhang, J. Combined effect of hindered amine light stabilizer and antioxidants on photodegradation of poly (vinyl chloride). *J. Thermoplast. Compos. Mater.* **2012**, *25* (7), 879−894.

(5) Wang, X.; Pan, H.; Yang, K.; Zhang, P. Cracking, structural, and mechanical property changes of SIBR and related elastomers during the ozone aging process. *Polym. Degrad. Stab.* **2022**, *195*, 109774.

(6) Allen, N. S.; Vasiliou, C.; Marshall, G. P.; Chen, W. Light stabiliser, antioxidant and pigment interactions in the thermal and photochemical oxidation of polyethylene films. *Polym. Degrad. Stab.* **1989**, *24* (1), 17−31.

(7) Wang, X.; Fang, K.; Xi, X.; Jia, D. Synthesis and anti-aging property in acrylonitrile-butadiene rubber of non-aromatic dendritic antioxidant with amine groups. *J. Macromol. Sci. A* **2017**, *54* (9), 612−621.

(8) Tuampoemsab, S. Influence of Amino Acids on Anti-Oxidative Properties of Green Natural Rubber and Natural Rubber Compound. *Adv. Mat Res.* **2013**, *747*, 664−667.

(9) Mars, W. V.; Fatemi, A. Factors that affect the fatigue life of rubber: A literature survey. *Rubber Chem. Technol.* **2004**, *77* (3), 391−412.

(10) Wu, S.; Qiu, M.; Guo, B.; Zhang, L.; Lvov, Y. Nanodot-Loaded Clay Nanotubes as Green and Sustained Radical Scavengers for Elastomer. *ACS Sustain. Chem. Eng.* **2017**, *5* (2), 1775−1783.

(11) Ouyang, C.; Wang, S.; Zhang, Y.; Zhang, Y. Improving the aging resistance of styrene−butadiene−styrene tri-block copolymer modified asphalt by addition of antioxidants. *Polym. Degrad. Stab.* **2006**, *91* (4), 795−804.

(12) Luo, K.; Zheng, W.; Zhao, X.; Wang, X.; Wu, S. Effects of antioxidant functionalized silica on reinforcement and anti-aging for solution-polymerized styrene butadiene rubber: Experimental and molecular simulation study. *Mater. Des.* **2018**, *154*, 312−325.

(13) Yang, J.; Lou, W. Molecule Dynamics Simulation of the Effect of Oxidative Aging on Properties of Nitrile Rubber. *Polymers* **2022**, *14* (2), 226.
(14) Contini, C.; Valzacchi, S.; O'Sullivan, M.; Simoneau, C.; Dowling, D. P.; Monahan, F. J. Overall Migration and Kinetics of Release of Antioxidant Compounds from Citrus Extract-Based Active Packaging. *J. Agric. Food Chem.* **2013**, *61* (49), 12155−12163.
(15) Bu, J.; Huang, X.; Li, S.; Jiang, P. Significantly enhancing the thermal oxidative stability while remaining the excellent electrical insulating property of low density polyethylene by addition of antioxidant functionalized graphene oxide. *Carbon* **2016**, *106*, 218−227.
(16) Zhao, S.; Li, J.; Yan, Z.; Lu, T.; Liu, R.; Han, X.; Cai, C.; Zhao, S.; Wang, H. Preparation of lignin-based filling antioxidant and its application in styrene-butadiene rubber. *J. Appl. Polym. Sci.* **2021**, DOI: 10.1002/app.51281.
(17) Wei, H.; Zhou, J.; Zheng, J.; Huang, G. Antioxidation efficiency and reinforcement performance of precipitated-silica-based immobile antioxidants obtained by a sol method in natural rubber composites. *RSC Adv.* **2015**, *5* (112), 92344−92353.
(18) Haider, N.; Karlsson, S. Kinetics of migration of antioxidants from polyolefins in natural environments as a basis for bioconversion studies. *Biomacromolecules* **2000**, *1* (3), 481−7.
(19) Ignatz-Hoover, F.; To, B. H.; Datta, R. N.; De Hoog, A. J.; Huntink, N. M.; Talma, A. G. Chemical additives migration in rubber. *Rubber Chem. Technol.* **2003**, *76* (3), 747−767.
(20) Brinkmann, M.; Montgomery, D.; Selinger, S.; Miller, J. G. P.; Stock, E.; Alcaraz, A. J.; Challis, J. K.; Weber, L.; Janz, D.; Hecker, M.; Wiseman, S. Acute Toxicity of the Tire Rubber-Derived Chemical 6PPD-quinone to Four Fishes of Commercial, Cultural, and Ecological Importance. *Environ. Sci. Technol. Lett.* **2022**, *9* (4), 333−338.
(21) Tian, Z.; Zhao, H.; Peter, K. T.; Gonzalez, M.; Wetzel, J.; Wu, C.; Hu, X.; Prat, J.; Mudrock, E.; Hettinger, R.; Cortina, A. E.; Biswas, R. G.; Kock, F. V. C.; Soong, R.; Jenne, A.; Du, B.; Hou, F.; He, H.; Lundeen, R.; Gilbreath, A.; Sutton, R.; Scholz, N. L.; Davis, J. W.; Dodd, M. C.; Simpson, A.; McIntyre, J. K.; Kolodziej, E. P. A ubiquitous tire rubber-derived chemical induces acute mortality in coho salmon. *Science* **2021**, *371* (6525), 185−189.
(22) Xie, H.; Li, H.; Lai, X.; Wu, W.; Zeng, X. Synthesis and antioxidative properties of a star-shaped macromolecular antioxidant based on β-cyclodextrin. *Mater. Lett.* **2015**, *151*, 72−74.
(23) Wang, X.; Wang, B.; Song, L.; Wen, P.; Tang, G.; Hu, Y. Antioxidant behavior of a novel sulfur-bearing hindered phenolic antioxidant with a high molecular weight in polypropylene. *Polym. Degrad. Stab.* **2013**, *98* (9), 1945−1951.
(24) Al-Ghonamy, A. I.; Barakat, M. A. Upgrading of acrylonitrile−butadiene copolymer properties using natural rubber−graft−N-(4-aminodiphenylether) acrylamide. *J. Appl. Polym. Sci.* **2010**, *118* (4), 2202−2207.
(25) Lu, M.; Liu, P.; Wang, F.; Ding, Y.; Zhang, S.; Yang, M. Synthesis of nanoparticle-immobilized antioxidants and their antioxidative performances in polymer matrices: a review. *Polym. Int.* **2018**, *67* (4), 356−373.
(26) Luo, K.; Ye, X.; Zhang, H.; Liu, J.; Luo, Y.; Zhu, J.; Wu, S. Vulcanization and antioxidation effects of accelerator modified antioxidant in styrene-butadiene rubber: Experimental and computational studies. *Polym. Degrad. Stab.* **2020**, *177*, 109181.
(27) Shi, K.; Ye, L.; Li, G. In situ stabilization of polyamide 6 with reactive antioxidant. *J. Therm. Anal. Calorim.* **2015**, *119* (3), 1747−1757.
(28) Lu, Y.; Yang, J.; Yin, D.; Tan, M.; Wang, J. Synthesis and aging properties of reactive antioxidant NAPM in natural rubber vulcanizates. *J. Appl. Polym. Sci.* **2008**, *108* (1), 576−582.
(29) Mora, A.-S.; Tayouo, R.; Boutevin, B.; David, G.; Caillol, S. Synthesis of biobased reactive hydroxyl amines by amination reaction of cardanol-based epoxy monomers. *Eur. Polym. J.* **2019**, *118*, 429−436.
(30) Susanna, A.; Armelao, L.; Callone, E.; Dirè, S.; D'Arienzo, M.; Di Credico, B.; Giannini, L.; Hanel, T.; Morazzoni, F.; Scotti, R. ZnO nanoparticles anchored to silica filler. A curing accelerator for isoprene rubber composites. *Chem. Eng. J.* **2015**, *275*, 245−252.
(31) Mathew, N. M.; De, S. K. Thermo-oxidative ageing and its effect on the network structure and fracture mode of natural rubber vulcanizates. *Polymer* **1983**, *24* (8), 1042−1054.
(32) Schmid, M.; Ritter, A.; Affolter, S. Determination of oxidation induction time and temperature by DSC - Results of round robin tests. *J. Therm. Anal. Calorim.* **2006**, *83* (2), 367−371.
(33) Zhong, B.; Shi, Q.; Jia, Z.; Luo, Y.; Chen, Y.; Jia, D. Preparation of silica-supported 2-mercaptobenzimidazole and its antioxidative behavior in styrene-butadiene rubber. *Polym. Degrad. Stab.* **2014**, *110*, 260−267.

https://doi.org/10.1021/acsomega.3c10301
ACS Omega 2024, 9, 15401−15409